Chemical Engineering & Processing: Process Intensification 129 (2018) 131–141

Contents lists available at ScienceDirect

Chemical Engineering & Processing: Process Intensification

journal homepage: www.elsevier.com/locate/cep

Potentiality of a biogas membrane reformer for decentralized hydrogen production

Gioele Di Marcoberardino*, Stefano Foresti, Marco Binotti, Giampaolo Manzolini

Politecnico di Milano, Dipartimento di Energia, via Lambruschini 4, 20156, Milano, Italy

ARTICLE INFO

Keywords:
Biogas
Hydrogen production
Membrane reactor
System efficiency
Economic analysis

ABSTRACT

This paper investigates the potentiality of membrane reactor for green hydrogen production from raw biogas. The assessment is carried out both from thermodynamic and economic point of view to outline the advantages of the innovative technology with respect to the conventional one based on reforming, water gas shift and pressure swing adsorption unit. Both biogas produced by landfill and anaerobic digestion are considered to evaluate the impact of biogas composition on system design.

BIONICO system model is implemented in Aspen Plus and Aspen Custom Modeler to perform respectively the balance of plant with thermal integration and a detailed fluidized bed membrane reactor design. Two permeate side configurations, sweep gas and vacuum pump, were modelled and compared. The adoption of membrane reactor increases the system efficiency by more than 20% points with respect to reference cases. Focusing on the economic results, hydrogen production cost show lower value respect to the reference cases (4 €/kg$_{H2}$ vs 4.2 €/kg$_{H2}$) at the same hydrogen delivery pressure of 20 bar. Between the landfill and anaerobic digestion cases, the latter has the lower costs as consequence of the higher methane content.

1. Introduction

Hydrogen is one of the most promising energy carrier that can replace fossil fuels providing low or near-zero greenhouse gases emissions energy. Its widespread deployment depends on the reduction of cost production and the use of renewable sources. Nowadays 96% of hydrogen comes from fossil fuels, in particular steam reforming of natural gas (NG) is the most used technology covering 50% of the global production [1,2]. At present, green hydrogen (hydrogen generated by renewable sources) production technology is limited to water electrolysis that, using photovoltaics or wind energy, is quite expensive [3–5]. One of the cheapest and promising way identified in the last years is the steam reforming of raw biogas (BG) [6], that mainly consists of methane and carbon dioxide. The conversion process can be similar to the one with natural gas but it should be scaled down to the typical existing biogas plants production size that is 100 times smaller [7]. Previous works have shown how this process is a technically and economically feasible technology for hydrogen production [8–10]. In general, H_2 can be produced by biogas steam reforming (BSR) in a wide temperature range between 600 and 1000 °C (endothermic and reversible reactions), involving catalytic processes that are often combined. Both reforming processes can be performed at low pressure (in most cases under atmospheric pressure) in tubular fixed bed or fluidized reactors [9,11–13]. The gas stream resulting from the conversion process is a mixture rich in hydrogen, so CO_2 and other pollutants must be removed through separation or sequestration (i.e. pressure swing adsorption unit [14]), affecting the capital expenditure of hydrogen production. Membrane reactor concept can strongly decrease volumes and footprint integrating the separation of hydrogen in situ together with the reforming reactions [15,16]. Moreover, membrane assisted reactor in fluidization regime are able to reduce bed-to-wall mass transfer limitation and smooth temperature profile even in the presence of strongly exothermic and endothermic reactions respect to fixed bed application [17,18].

The BIONICO project focuses on the adoption of fluidized membrane reactor to produce green hydrogen from biogas to produce 100 kg/day of pure hydrogen [19]. The advantages of the adoption of membrane reactor for biogas steam reforming can be found in literature at lab-scale, using mixtures of CO_2 and CH_4 to mimic the biofuel compositions, while limited number of cases using real biogas from the direct digestion process of residual biomass [13,20–22]. Therefore the success of BIONICO technology, that will be installed in a real biogas plant production, will reduce the hydrogen production costs when using biogas as feedstock favouring hydrogen penetration into the market.

This work performs a techno-economic assessment of the innovative

* Corresponding author.
E-mail address: gioele.dimarcoberardino@polimi.it (G. Di Marcoberardino).

https://doi.org/10.1016/j.cep.2018.04.023
Received 11 August 2017; Received in revised form 19 April 2018; Accepted 20 April 2018
Available online 25 April 2018

Nomenclature

$\Delta H^0_{298\ K}$	Heat of reaction in standard conditions, kJ/mol
A_{mem}	Membrane area, m^2
E_a	Energy activation, kJ/mol
k_0	Pre exponential factor, $mol/smPa^n$
k'	Permeance, mol/sm^2Pa^n
n	Exponential factor, –
$\dot{n}_i$	Molar flow, kmol/s
P	Pressure, bar
p_i	Partial pressure, bar
T	Temperature, °C
W_{aux}	Electric auxiliary consumptions, kW
x_i	Molar fraction, –

Acronyms

AD	Anaerobic digester
ATR	Autothermal reformer
ATR-MR	Autothermal membrane reformer
BG	Biogas
BSR	Biogas steam reforming
CAPEX	Capital expenditure
C&OC	Owner's and contingencies costs
CCF	Capital charge factor
D	Diameter, m
EU	Europe
HT	High temperature
HX	Heat exchanger
IC	Indirect costs, €
LCOH	Levelized cost of hydrogen, €/kg
LF	Landfill
LHV	Low heating value
LT	Low temperature
NBS/NRC	National Bureau of standards/ Nucleare Regulatory Commission
NG	Natural gas
O&M	Operation and maintenance costs, €
OPEX	Operating expenditure
P	Pump
PSA	Pressure swing adsorption unit
S/C	Steam to carbon molar ratio, –
SR	Steam reformer
TEC	Total Equipment Cost, €
TIC	Installation costs, €
TPC	Total Plant Cost, €
TSA	Temperature swing adsorption unit
VPSA	Vacuum Pressure swing adsorption unit
WGS	Water gas shift

Subscripts

in or feed	ATR-MR inlet
perm	ATR-MR permeate side
ret	ATR-MR retentate side
mem	Membrane

Greek letters

η_{sys}	System efficiency in terms of LHV of hydrogen, %
λ_{ATR}	Air to flow to ATR inlet ratio, –
$\eta_{el,ref}$	Average electric efficiency of the power generating park, %

system for green hydrogen production from biogas based on autothermal fluidized bed catalytic membrane reactor. The assessment is carried out through detailed modelling of the innovative system to perform respectively the balance of plant with thermal integration and a detailed fluidized bed membrane reactor design. Results were compared with two conventional technologies: steam reforming (SR) and autothermal reforming (ATR). The former represents the most diffused system, while the second is closer to the technology developed within the BIONICO project. In both cases, the reforming reactor is followed by two temperature-staged water gas shift reactors and a pressure swing adsorption system (PSA). One of the main parameters that must be taken into consideration when dealing with biogas for the reforming process is the biogas composition. Biogas usually contains from 45% to 70% methane and from 30% to 45% carbon dioxide but can also contain nitrogen, hydrogen sulphide, halogenated compounds and organic silicon compounds. BIONICO system should improve performances of actual conventional systems as well as reducing hydrogen production cost.

2. Conventional hydrogen production from biogas

As biogas composition is quite similar to natural gas, steam reforming (SR) and autothermal reforming (ATR) plants have been identified as benchmark for hydrogen production from biogas. Fuel processors chain also include one or two stages of water gas shifts to enhance hydrogen concentration in the reformate stream and a pressure swing adsorption unit for hydrogen separation and purification, as shown in Fig. 1. Detailed methodology and results, together with main assumptions and parameters, can be found in [14]. The PSA for small scale applications usually includes four beds and have a limited hydrogen recovery to achieve the target purity (> 99.99%). For this reason, a LT-WGS is adopted to increase the hydrogen concentration with advantages for the PSA operating conditions and the overall system efficiency.

The two SR and ATR plants were configured in Aspen Plus, integrating the VPSA model studied, and analysing the behaviour of the systems at the variation of the pressure and the type of input biogas. The size of the considered hydrogen production plant is equal to the target of BIONICO project and equal to 100 kg/day with a pressure delivery of 20 bar. Fig. 2 and Table 1 summarize main results of the best configuration of the conventional system in terms of system efficiency and hydrogen production cost. The SR system achieves a maximum efficiency, calculated on the LHV, of 52% at 12 bar, while the ATR of 28% at 18 bar. The economic analysis determined a hydrogen production cost of around 5 €/kg of hydrogen with the SR concept.

3. Methodology

3.1. General assumptions and definitions

The innovative fuel processor and their relative balance of plant are implemented in Aspen Plus® [23], where mass and energy balances are solved. The methodology adopted is consistent with previous works [24–26]. The Peng-Robinson cubic equation of state [27] is used for all thermodynamic properties except for liquid molar volume evaluation where the Rackett model [28] is used and for steam properties where NBS/NRC steam tables [29] are adopted. A specific phenomenological model of membrane reactor developed in Aspen Custom Modeler® (ACM) [23] was adopted: it is described extensively in Section 3.2.[1]

BIONICO system is designed to produce 100 kg/day of pure

[1] The code for the membrane reactor modelling is confidential

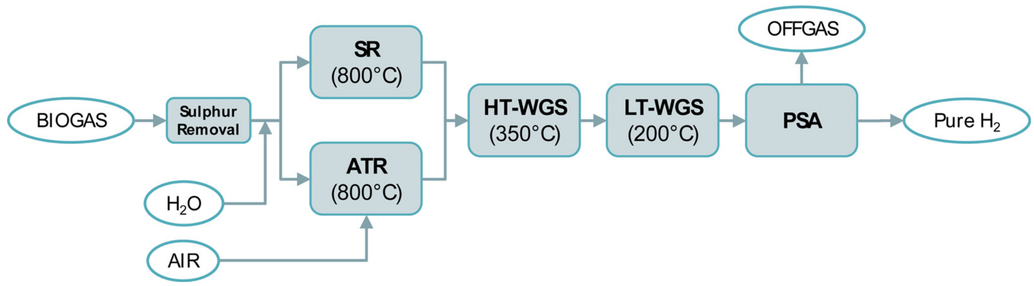

Fig. 1. Process flow diagram of reference configurations for hydrogen production from biogas.

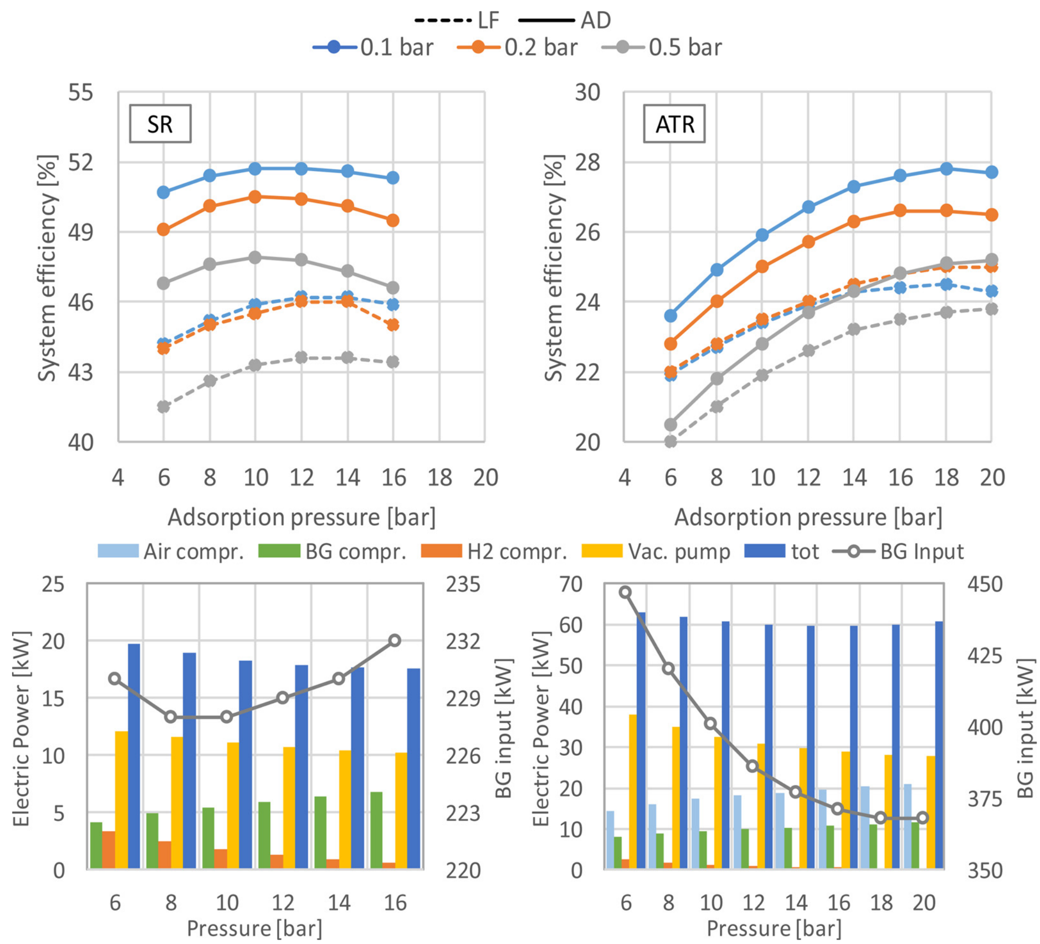

Fig. 2. Top: system efficiency for SR (left) and ATR (right) cases. Bottom: Auxiliary consumptions for the best case with AD BG and VPSA pressure 0.1 bar for SR (left) and ATR (right).

hydrogen. This work sets a pressure delivery of 20 bar to compare the system efficiency with the conventional plants (an additional hydrogen compressor is introduced since hydrogen stream is produced at ambient pressure). Moreover, the impact of a higher final hydrogen delivery pressure for refuelling stations (i.e. 700 bar) has also been analysed. The design parameters and the main assumptions of the reference cases are summarized in Table 2. The auxiliary values adopted for the balance of plant (BoP) result from benchmark technologies, typical O&M specifications, requirements for the materials.

All the cases are compared in terms of overall system efficiency, defined in Eq. (1) as the ratio of H_2 energy output to biogas and auxiliaries energy inputs:

$$\eta_{sys} = \frac{\dot{m}_{H_2} LHV_{H_2}}{(\dot{m}_{BG,f} + \dot{m}_{BG,aux}) LHV_{BG} + {}^{W_{aux}}/_{\eta_{el,ref}}} \tag{1}$$

where:

- LHV_{H_2} is equal to 120 MJ/kg ;
- W_{aux} is the sum of the electric consumptions of the system auxiliaries (i.e. compressors, pumps, control system);
- $\eta_{el,ref}$ is set equal to 45%, as the average electric efficiency of the power generating park.

The steam to carbon ratio (S/C), defined as the steam molar flow rate to methane molar flow rate, is fixed at the beginning of the membranes region (see Section 3.2) after the partial oxidation where the amount of water and methane is respectively higher and lower respect to the reactor inlet. The air flux is calculated in Eq. (2) balancing the heat required by the endothermic reforming reaction and to maintain the reactor operating temperature.

Table 1
Main results of performance and hydrogen production cost for conventional fuel processors.

Parameter	units	SR		ATR	
BG composition	–	LF	AD	LF	AD
S/C	–	4	4	3	3
p	bar	14	12	18	18
H_2 production / delivery pressure	kg/day / bar	100/20	100/20	100/20	100/20
BG Feed	Nm^3/h	56.1	39.5	92.4	63.5
BG Input	kW	247	229	407	368
Tot aux consumptions	kW	24.3	17.9	73.0	60.0
System efficiency @ 20 bar	%	46.2	51.7	24.5	27.8
TPC	k€	199.0	175.1	235.5	226.0
O&M (fixed and variable)	k€/y	117.1	117.4	181.2	176.8
LCOH (H_2 @20 bar)	€/kg	4.29	4.21	6.60	6.41
LCOH (H_2 @700 bar)	€/kg	5.09	4.97	7.32	7.14

Table 2
Reference case model assumptions and design parameters.

Parameter	units	value[a]
Feed & operating conditions		
Uniform fluidized bed reforming temperature	°C	550 (500-600)
Pressure reaction side	bar	12 (8-16)
Pressure permeate side vacuum/sweep	bar	0.1 (0.1-0.3) / 1.1
S/C ratio at the beginning of membranes region	–	3 (2.5-3.5)
u/umf at reactor inlet	–	2.5 - 3.5
Excess air to burner	%	100
$\lambda_{ATR\text{-}MR}$ (air to ATR-MR)	–	≈ 0.3
Sweep to CH_4 ratio	molar	1.5 - 2.5
Ambient temperature	°C	15
Vented gas temperature	°C	60
H_2 production target	kg/day	100
H_2 delivery pressure	bar	20
Heat Exchangers and thermal dissipations		
Design minimum ΔT in exchangers gas/gas	°C	30
Design minimum ΔT in exchangers gas/liquid	°C	30
Design minimum ΔT in exchangers liquid/bi-phase	°C	15
Heat losses in HX's (fraction of thermal duty)	%	1-5
Heat transfer coefficient gas/gas	W/m^2K	60
Heat transfer coefficient gas/liquid or bi-phase	W/m^2K	70
Auxiliaries & controls		
Pumps hydraulic efficiency	%	70
Pumps driver mechanical efficiency	%	90
Compressors/fans isentropic efficiency	%	70
Compressors/fans motor mechanical efficiency	%	85
BG compressor maximum outlet temperature	°C	120
Controller consumption (% of total auxiliary consumptions)	%	10
Vacuum pump		
Isentropic efficiency	%	70
Motor mechanical efficiency	%	85
Inlet pressure	bar	0.1 (0.1–0.2)
Discharge pressure	bar	1.2
Maximum outlet temperature	°C	70

[a] Where a range of interest is shown between brackets, the most likely value is indicated separately.

$$\lambda_{ATR-MR} = \frac{\dot{n}_{AIR}}{\dot{n}_{O_2,ST}/x_{O_2,AIR}} \tag{2}$$

The impact of BG type was investigated considering two different compositions that are reported in Table 3 [30]. The first, coming from landfill, has less CH_4 and higher inert content while the second, from anaerobic digester, has a high CH_4 content resulting in a highest LHV value. The BG fee is exempt of sulphur content: a cold sulphur compound removal unit with activated carbon is so neutral to the purpose of the model.

3.2. Fluidized bed autothermal membrane reactor model

The importance of developing a phenomenological model of the membrane reactor implementing detailed transport phenomena in the membrane reactor was demonstrated in a previous work: the calculated membrane area of the detailed can be up to 50% higher than the one calculated with an ideal approach [31]. Advantages of ACM are the implementation of custom component in Aspen Plus avoiding the use of multiple environments, the fast coding (that allows a quick switch of the problem from design to simulation conditions by changing the "state" of the variables of the problem) and the computation of thermodynamic and transport properties of the species or mixtures by calling a large variety of internal sub-routines; main drawback is the poor control of the user on the solving procedure (e.g. there are no debug functions). The model was validated against experimental results as well as another well-established approach used as reference [32].

The model includes reforming reactions (different kinetic schemes or chemical equilibrium), detailed hydrodynamics of bubble-emulsion phases and different options on the permeate side (vacuum or co-counter flow sweep gas, including gas diffusion limitations in the porous support). Membrane reactor bed is divided into three main regions, which lengths can be set by the user: the first region at the bottom of the reactor is dedicated to the oxidation and reforming reactions, the middle region is occupied by the membranes (permeation zone); the last section is a buffer region that mainly corresponds with the free-board region [33]. The schematic of ACM fluidized bed membrane reactor model is depicted in Fig. 3 while the main features of reactor design are reported in Table 4.

Fluidized bed fluid-dynamic correlations are substantially the same as in the model developed by TU/e [31]. The complete list of mass and energy balances, and fluid-dynamic equations for the bubbling bed are listed in [32]. The Aspen model includes also a global energy balance between the bed, the permeate stream, and the surroundings. The energy balance assumes a perfectly isothermal bed and energy transfer with the ambient is accounted for by heat conduction across the insulation thickness of the reactor and with the permeate side by heat conduction across the submerged membrane tubes and by the material flow of hydrogen.

The schemes of reactions implemented are steam reforming (R.1), water gas shift (R.2) and methane oxidation (R.3), with kinetic laws from [34] and [35] respectively. The model neglects carbon deposition as there is no kinetic law available for the considered catalyst. However, the high S/C ratio, the autothermal condition and the CO_2 content should prevent carbon deposition [36,37]. Solids can be distinguished between the catalyst and the filler material. The filler is chemically inert, made of the same material as the support of the catalyst. Only spherical particles with the nominal diameter are considered.

$$CH_4 + H_2O \Leftrightarrow CO + 3\,H_2 \quad \Delta H^0_{298\,K} = 206\ \text{kJ/mol} \tag{R.1}$$

$$CO + H_2O \Leftrightarrow CO_2 + H_2 \quad \Delta H^0_{298\,K} = -41\ \text{kJ/mol} \tag{R.2}$$

$$CH_4 + 2\,O_2 \Rightarrow CO_2 + 2\,H_2O \quad \Delta H^0_{298\,K} = -802\ \text{kJ/mol} \tag{R.3}$$

Table 3
Investigated biogas compositions.

Species	units	Landfill	Anaerobic Digester
CH_4	%mol	44.2	58.1
CO_2		34.0	33.9
N_2		16.0	3.8
O_2		2.7	1.1
H_2		0.0165	–
CO		0.0006	–
H_2O		Saturated	Saturated
p / T	bar / °C	1.013 / 25	1.013 / 25
LHV	MJ/kg	12.7	17.8

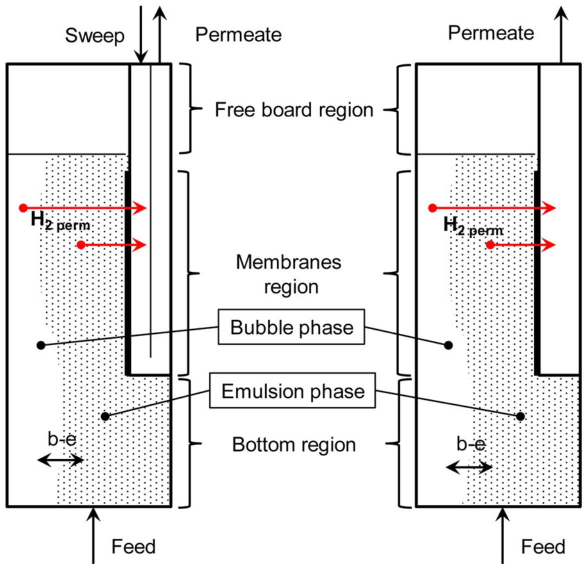

Fig. 3. Scheme of fluidized bed membrane reactor developed in ACM for vacuum pump and sweep gas case.

Table 4
ACM membrane reactor geometry parameters.

Parameter	units	value
L reactor	m	1
L bottom region (from distributor to membrane)	m	0.1
L free board region	m	0.45
D reactor	m	0.44–0.6
Membrane distance	m	0.01–0.026

Performance of the membrane reactor can be expressed in terms of the Hydrogen Recovery Factor (HRF), defined in Eq. (3) as the ratio between permeated hydrogen and the maximum amount of hydrogen that could be produced.

$$HRF = \frac{\dot{n}_{H_2,perm}}{4\cdot\dot{n}_{CH_4,ret} + \dot{n}_{CO,ret} + \dot{n}_{H_2,ret} + \dot{n}_{H_2,perm}} = \frac{\dot{n}_{H_2,perm}}{4\cdot(\dot{n}_{CH_4,in} - 2\dot{n}_{O_2,in})} \tag{3}$$

Membranes consist of a Pd-Ag layer deposited onto a ceramic multilayer porous support. Parameters of the permeation law (Eq. (4)) (pre-exponential factor k_0, apparent activation energy E_a and exponential factor n), listed in Table 5, comes from experimental analysis of [22]. Hydrogen is assumed to be extracted from both the bubble and the emulsion phase, weighted on the local phase composition and extension of the two phases. Gas diffusion in the support is modelled by simplified Stefan-Maxwell equations and affect results just for the sweep gas case: the pressure gradient is neglected and the effective gas diffusivity includes both the molecular and Knudsen diffusion contributions. The equations applied to a two-species mixture (hydrogen and the sweep gas) reduce to Fick's law for non-stationary media and are then integrated for the specific case of cylindrical geometry. A thorough description of the model, definitions and assumptions can be found in [32].

$$\dot{n}_{H_2,perm} = k_0 e^{\frac{-E_a}{RT}} \frac{(p_{H_2,feed}{}^{n} - p_{H_2,perm}{}^{n})}{\delta} A_{mem} = k' (p_{H_2,feed}{}^{n} - p_{H_2,perm}{}^{n}) A_{mem} \tag{4}$$

The considered membranes can withstand temperatures up to 550 °C without loss of selectivity and absolute pressure difference between feed and permeate sides of 20 bar [38,39]. The main issue about membrane with biogas is towards sulphur tolerance which is really limited. However, a commercial active carbon bed is enough to remove the H_2S content in the biogas below critical concentration for the membrane [40].

3.3. BIONICO system layouts

Two BIONICO system configurations, which differ for the permeate side, are investigated enhancing the hydrogen separation. The first one considers a vacuum pump at the permeate outlet, reducing the permeate total pressure while using steam as sweep gas allows the reduction of the hydrogen partial pressure. In the vacuum pump case, the reactor requires simpler constructive techniques and less welded joints (i.e. lower reactor costs and probably higher reliability), but infiltrations might occur in the plant section below atmospheric. The adoption of sweep stream reduces auxiliaries' power consumption (i.e. vacuum pump is replaced by a water pump) increasing the complexity of the membrane reactor.

3.3.1. BIONICO layout using vacuum pump

The vacuum pump configuration is shown in Fig. 4. The BG is firstly compressed in CMP_{BG}, then preheated up to 300 °C in HX-4. It is mixed with steam and water at the inlet of the ATR-MR. At the ATR-MR outlet, the retentate (point 3) and hydrogen (point 6) leave from the top section of the reactor. The retentate stream, which mainly consists of steam, CO_2 and N_2 with the remaining CO, CH_4 and H_2 is cooled down to 200 °C (point 4) where it is throttled before being combusted in air. The thermal power released during retentate and permeate cooling is used for steam production (HX-1, HX-2 and HX-3). The exhaust gases (point 5) are cooled down in a dry cooler recovering process water to minimize the make-up for the reforming reaction; water make-up is an additional operating cost. The separated hydrogen is cooled down to 30 °C (thanks to the heat sink HXD-1), and then compressed to the delivery pressure by the vacuum pump. The amount of hydrogen separated in the ATR-MR is determined so that the thermal power of the retentate close the energy balance of the system avoiding additional BG supply. Table 6 summarizes the thermodynamic properties of the main streams involved for one of the simulation case with landfill biogas.

3.3.2. BIONICO layout using sweep gas

The same system with the adoption of sweep gas in the membrane reactor (sweep gas case) is depicted in Fig. 5. With respect to the vacuum pump case, the layout is more complex because additional heat exchangers are required to evaporate the sweep gas steam (HX-6, HX-7, HX-8). Liquid feed water evaporated through HX-1 and HX-2 and finally superheated in HX-4 together with biogas. At the inlet of the reactor a preheated mix of compressed BG and steam (point 1) and compressed air (point 2) feed the reactor from the bottom section while steam for sweep gas is fed separately. At the outlet, the retentate (point 3) and hydrogen (point 6) leave from the top section of the reactor. After cooling down, the remaining fuel in the retentate (point 4) is combusted in the burner for the steam generation. The sweep gas steam is evaporated thanks to the exhaust gas thermal power and superheated using the permeate stream. The process water is recycled from the condensation in all the three separators downstream the cooling of the

Table 5
Membrane features.

Parameter	units	value
OD/ID	m	0.014/0.007
Support thickness	m	0.0035
Length	m	0.45
Membrane thickness (δ)	μm	4.5
k_0	$mol\ s^{-1}\ m^{-1}\ Pa^{-n}$	$3.93\ 10^{-8}$
E_a	$kJ\ mol^{-1}$	9.26
n	–	0.5

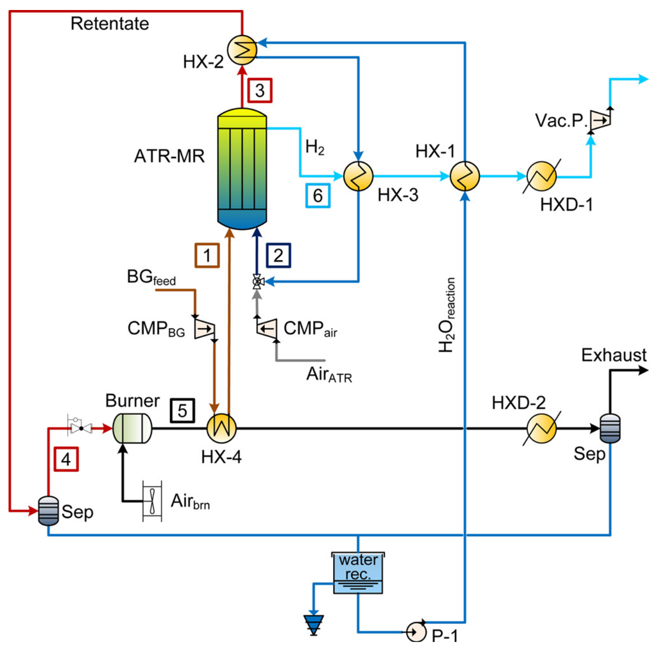

Fig. 4. Layout of BIONICO system using vacuum pump.

permeate, retentate and exhaust gases. Table 7 summarizes the thermodynamic properties of the main streams involved for one of the simulation case with landfill biogas.

4. System performance

4.1. Membrane reactor design

Integration of the phenomenological membrane reactor model in the overall system Aspen Plus model has two significant effects, compared to previous works [24,41]: (i) evaluation of the influence of kinetic and transport phenomena in fluidization on hydrogen recovery factor (or reactor efficiency) and (ii) the definition of the main reactor design parameters such as reactor diameter (D reactor), average membrane distance (Mem. Dist.) or required membrane area.

A sensitivity analysis on the reactor design parameters was carried out at different operating conditions (reactor pressure and temperature, S/C and permeate pressure), for both LF and AD biogas and both permeate side configuration, in order to identify the minimum required membrane keeping a good system efficiency and a u/u_{mf} ratio at reactor inlet of about 3 (within the range of 2.5–3.5). Lower gas velocities are not enough to guarantee a good fluidization regime along the reactor while higher values increase the gas fraction flowing though the bubble phase causing a by-pass effect in the membrane region. This turns out in lower hydrogen production and separation.

Fig. 6 shows results of BIONICO system with vacuum pump fed with landfill biogas at 550 °C, 12 bar, S/C 3 and 0.1 bar on the permeate side. System efficiency together with the resulting u/u_{mf} ratio at different reactor size and membrane distance (or amount of membranes) are plotted as a function of the required membrane area to produce 100 kg/day of pure hydrogen. System performance is almost constant for membrane area bigger than 3 m^2, beyond which it quickly decreases. Starting from an efficiency value of about 71.5% that corresponds to a membrane are of about 3.5 m^2, the corresponding reactor diameter of 0.48 m and membrane distance of 0.018 m can be found in reactor size grid checking that even the u/u_{mf} ratio is respected.

Therefore this tool allows to identify the best compromise between system efficiency and reactor design for each operating conditions as further discussed below.

4.2. BIONICO system performance using vacuum pump

This section reports the system efficiency results for the BIONICO concept using both LF and AD biogas. Respect to the reference cases, the membrane reactor produces hydrogen at low pressure. Preliminary results are calculated assuming a H_2 delivery pressure of 1.2 bara, and efficiency variation curve as function of the delivery pressure will be shown at the end of this section. Figs. 7 and 8 report the system efficiency for the vacuum pump case using LF BG and AD BG as feedstock respectively. In general, the BIONICO system can achieve hydrogen production efficiencies in the range of 70–74%. The highest efficiency is achieved when AD BG is used as feedstock thanks to the higher methane concentration.

The advantages of a higher CH_4 concentration are more evident from the membrane surface area which reduces by 10% (3.5 m^2 for LF BG vs. 3.17 m^2 for AD BG) rather than system efficiency. In the same figure, the system efficiency and membrane surface area are determined for different reactor operating conditions. The following consideration can be drawn for both cases:

- Reactor temperature reduction has negligible impact on the system efficiency thanks to the low heat required for self-sustaining reforming reactions, but it drastically affects the membrane surface area. At 500 °C, membrane surface area increases by 85–90% mainly because of the lower hydrogen production (less methane conversion) and lower permeance value k' (see Eq. (4)). On the other hand, an increase of operating temperature (600 °C) enhances permeance value and hydrogen production by reforming reaction reducing the required membrane area but also the hydrogen recovery factor (see Fig. 9), thus system efficiency is lower. High dilution of hydrogen on the retentate side due to the increase of inert in the reactants streams (air for partial oxidation) has a high impact on LF BG respect to the AD BG where the methane concentration is higher.
- The permeate pressure has a significant impact on the membrane area (and on system efficiency only for AD BG), while the feed pressure has limited impacts. Considering the opposite trends between the system efficiency and membrane area, the optimal operating condition will be identified using the economic assessment.
- Regarding the S/C, reducing the steam (S/C 2.5), the membrane area increases because of the lower reactant concentration which penalizes product formation (H_2). An opposite trend can be noticed

Table 6
Vacuum pump case: stream properties at in/exit of reactors (@pressure and T).

Stream	Flow		T (°C)	p (bar)	Composition (% molar basis)						
	Molar (mol/s)	Mass (g/s)			CH_4	H_2	CO	CO_2	H_2O	O_2	N_2
1	0.44	12.25	282.6	12	44.2	–	–	34.0	3.1	2.7	16
2	0.66	15.97	467	12	–	–	–	–	43.6	11.8	44.6
3	0.82	27.1	550	12	0.05	0.9	0.41	0.9	12.6	–	44.6
4	0.82	27.1	230	12	0.05	0.9	0.41	0.9	12.6	–	44.6
5	0.99	32.07	312.7	1.1	–	–	–	34.8	11.3	2.9	51.0
6	0.58	1.17	550	0.1	–	100	–	–	–	–	–

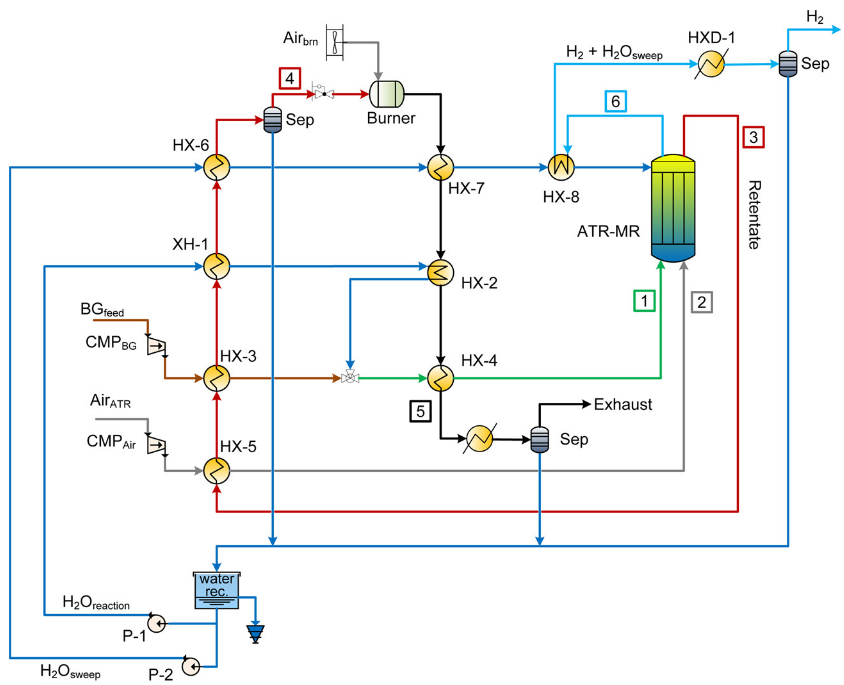

Fig. 5. Layout of BIONICO system using sweep gas.

Table 7
Sweep gas case: stream properties at in/exit of reactors (@pressure and T).

Stream	Flow		T (°C)	p (bar)	Composition (% molar basis)						
	Molar (mol/s)	Mass (g/s)			CH_4	H_2	CO	CO_2	H_2O	O_2	N_2
1	1.16	27.35	535	20	24.9	–	–	19.2	45.4	1.5	9.0
2	0.32	9.32	520	20	–	–	–	–	–	21	79
3	1.24	35.51	550	20	6.4	5.4	2.0	32.9	24.3	–	29.1
4	0.9	28.29	30.1	20	8.6	7.4	2.7	41.1	0.2	–	39.9
5	2.32	70.76	335	1.1	–	–	–	20.2	9.6	4.7	65.5
6	1.15	11.56	550	1.1	–	50.0	–	–	50.0	–	–

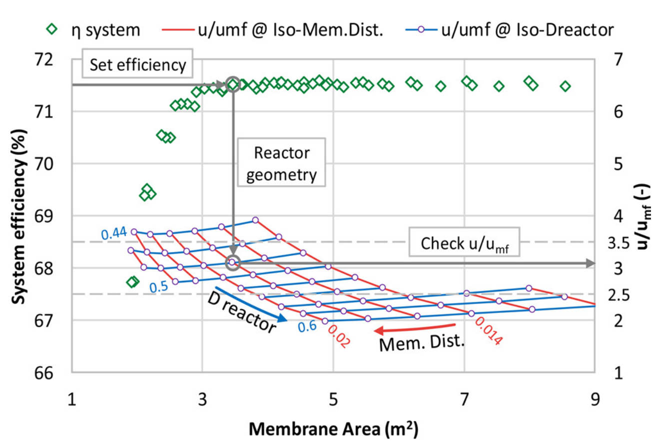

Fig. 6. Example of system efficiency and u/u_{mf} for LF BG using vacuum pump (550 °C, 12 bar, S/C 3, 0.1 bar) at different reactor design (Membrane Area (m^2), Reactor diameter (m) and membrane distance (m)).

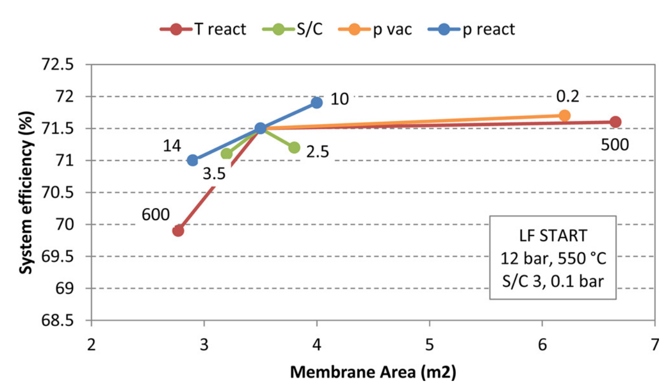

Fig. 7. BIONICO system performance using vacuum pump with LF BG.

for the two BG compositions as consequence of the different inert contents in BG stream. However, to prevent carbon deposition, the S/C ratio of 3 is considered the most interesting case.

4.3. BIONICO system performance using sweep gas

Results for the sweep case are reported in Figs. 10 and 11. The sweep gas case has lower performance and larger membrane area with respect to the vacuum pump case. The sweep gas pressure is set at 1.1 bar (slightly higher than the atmospheric pressure) leading to limited hydrogen partial pressure between the feed and the permeate side with the amount of sweep gas flowrate available. The gas diffusion in the porous support has a significant impact on the system efficiency where values above 50% can be obtained for higher pressure (16–20 bar) respect to the vacuum pump analysis (under 16 bar, system is not able to reach the BIONICO target). At high pressure, the benefits of higher hydrogen mass transfer in the support are larger than the increase of auxiliary consumptions. Fig. 11 show as working at low

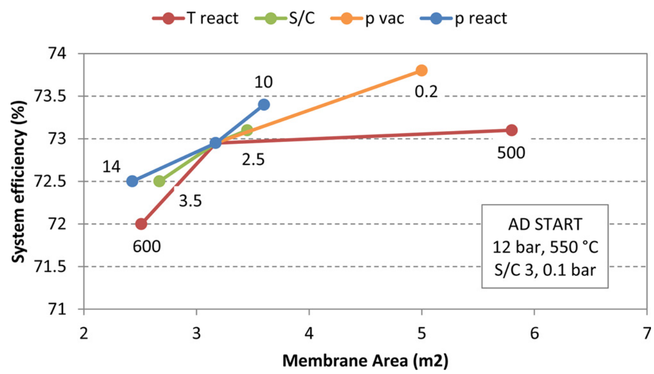

Fig. 8. BIONICO system performance using vacuum pump with AD BG.

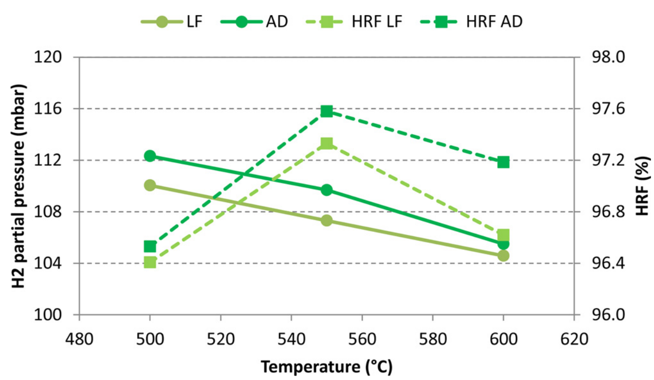

Fig. 9. Retentate hydrogen partial pressure (reactor exit) at different operating temperature.

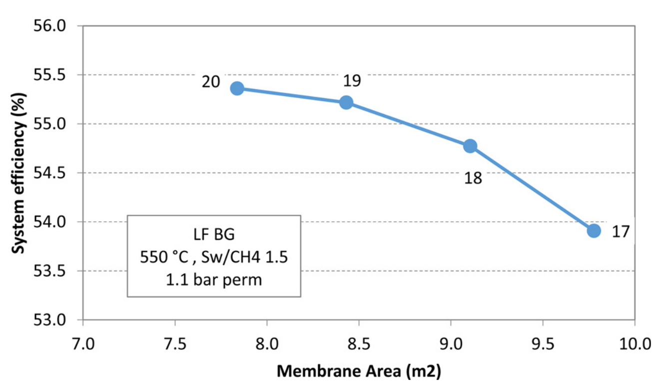

Fig. 10. BIONICO system performance using sweep gas.

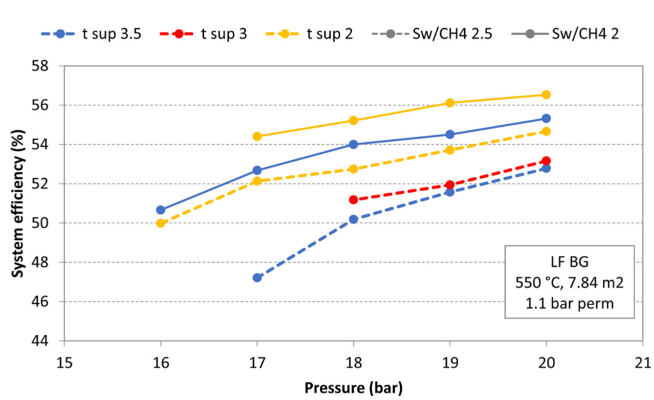

Fig. 11. BIONICO system performance using different amount of sweep gas and different support thickness.

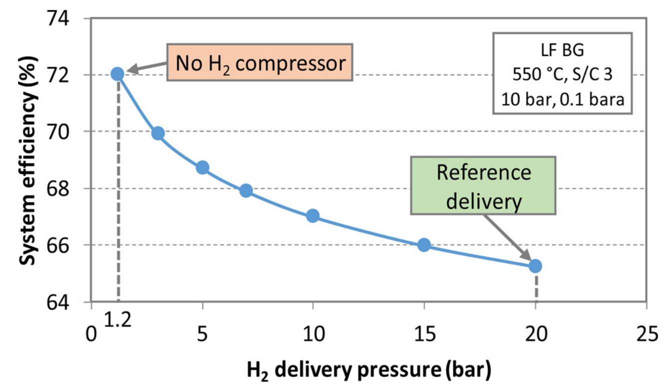

Fig. 12. Example of H_2 compressor consumption impact on BIONICO system efficiency.

sweep mass flow rate increases the pressure efficiency due to the less heat required for steam evaporation while decreasing the support thickness (from 3.5 mm to 2.0 mm) has advantages on system efficiency.

4.4. Results comparison

The impact of H_2 delivery pressure on the system efficiency is reported in Fig. 12. The H_2 compression significantly affects the system efficiency with a reduction around 9.4% when H_2 delivery pressure of 20 bar is considered (consistent to the reference cases (see Section 2)). Anyway, the overall system efficiency for the BIONICO system is 65.2% which is 19 and 41 percentage points higher than SR and ATR cases assumed as reference respectively.

Finally, the power balances of the most interesting cases considered are summarized in Table 8.

5. Economic analysis

Starting from the thermodynamic results, a preliminary economic analysis of BIONICO systems configurations is carried out to compare cost of produced hydrogen at different operating conditions. Results are also compared with values found for the conventional hydrogen production system from biogas in section 2 and [14].

The total plant cost (TPC) is calculated with the bottom-up approach breaking down the power plant into the basic components or equipment, and then adding installation costs, indirect costs and owner's and contingencies costs [42]. The components costs, obtained

Table 8
Power balances for the most interesting cases of the BIONICO system.

Parameter	units	BIONICO LF			BIONICO AD	
Temperature	°C	550	550	550	550	550
S/C	–	3	3	3	3	3
P feed	bar	12	10	20	12	12
P permeate	par	0.1	0.1	1.1/sweep	0.1	0.2
BG Feed	Nm^3/h	35.2	35.3	50.8	26.8	27.1
BG Input	kW	154.6	155.0	223.3	154.8	156.7
H_2 production	kg/day	100	100	100	100	100
System efficiency	%	71.51	71.90	55.36	72.99	73.83
System efficiency (H_2 @ 20 bar)	%	65.1	65.2	51.2	66.1	66.7
System efficiency (H_2 @ 700 bar)	%	56.2	56.4	45.6	57.0	57.5
BG compressor	kW	4.5	4.3	7.4	3.4	3.5
Air compressor	kW	4.9	4.7	4.1	5.3	5.3
H_2 vacuum pump	kW	6.4	6.4	–	6.4	4.1
H_2 compressor @ 20 bar	kW	9.0	9.0	9.0	9.0	9.0
H_2 compressor @ 350 bar	kW	17.4	17.4	17.4	17.4	17.4
H_2 compressor @ 700 bar	kW	24.1	24.1	24.1	24.1	24.1

from several literature sources, quotes and reports are then scaled and actualized with the CEPCI index method.

To evaluate the final cost of hydrogen (LCOH), consumables, auxiliaries and fixed are added to the TPC, according to the following formulation:

$$\boldsymbol{LCOH} = \frac{(\boldsymbol{TPC} * \boldsymbol{CCF}) + \boldsymbol{C}_{\boldsymbol{O\&M_{fix}}} + (\boldsymbol{C}_{\boldsymbol{o\&M_{var}}} * \boldsymbol{h_{eq}})}{\boldsymbol{kg}_{\boldsymbol{H_2}}(\boldsymbol{or\ Nm}^3_{\boldsymbol{H_2}})} \quad (5)$$

where the operating hours of the plant have been taken equal to 7500, while the CCF have been taken equal to 16%. Methodology and components costs are described in detail in [14]. The total installation costs were taken as 65% more than the total equipment cost (instead of 80% of the conventional systems [14]) due to the higher compactness and simplicity of the layout (3 reactors and PSA are replaced with one single component).

The palladium membranes on the ceramic support cost is retrieved from previous project [43] and refers to a production at a semi-industrial scale: cost of membrane is included both in the capital cost and in the O&M variable costs taking into account a lifetime of 5 years. About ATR-MR reactor cost, reactor is a 316 Stainless steel pressurized vessel whose volume is a result of ACM model. The heat exchangers are in counter-current configuration with hot gas flow externally to staggered stainless steel tubes bundle. The exchange areas of the heat exchangers have been calculated starting from the temperatures and exchanged power calculated from Aspen Plus, using typical heat transfer coefficients for gas/gas, gas/liquid and liquid/bi-phase that are defined in Table 2.

Table 9 reports the O&M fixed and variable costs that are represented by consumables (catalyst, biogas, water and membranes), auxiliaries, maintenance, insurance and operators cost. In particular, BIONICO catalyst, whose quantity is defined by ACM model (50% catalyst and 50% filler particles), has an higher specific cost respect to the conventional reforming catalyst since PGM particles are used.

5.1. Results

First, the equipment costs and the related TPC of the most interesting cases analysed, are evaluated. Table 10 summarizes the best case with a reactor temperature of 550 °C and S/C of 3.

From a TPC point of view, the advantages of BIONICO system depend on the investigated biogas composition and on the adopted operating conditions: the membranes cost has the largest influence on the total plant cost while the difference in auxiliary cost is limited. So the ATR-MR reactor configuration becomes favourable for high operating pressure and for AD biogas: this is because of the lower number of membrane required, due to the higher methane content in the biogas. The overall cost of the hydrogen compressor used to bring the delivery pressure of hydrogen from 1.2 bar to 20 bar (or 700 bar) have the same influence on TPC for all the cases, since the pressure ratio required is constant. The sweep gas case avoid the vacuum pump cost but all the other components have an higher cost due to the low system efficiency that is reflected on higher biogas flow and required membrane area.

Considering the different auxiliaries consumption and needs, the O&M variable costs were determined. Table 11 summarizes the singular contributes for the following cases.

Finally, Fig. 13 compares the levelized cost of hydrogen of reference and innovative solutions. The total cost is split in capital expenditure (CAPEX) and both fixed and variable operating expenditure (OPEX) for hydrogen delivery pressure of 20 bar. The term H_2 compression accounts for the installation and the electric energy consumption in case of a delivery pressure of 700 bar. The BIONICO concept seems to be cheaper than the reference system in all the cases using vacuum pump. When adopting AD biogas, the cost of hydrogen is lower than the one for the production by LF due to the highest efficiency and the lowest required membrane area. The major costs are the membrane reactor, therefore higher pressure are beneficial, and the heat exchangers for the thermal integration and also the variable O&M costs, due to the higher electricity consumption and catalyst cost. In general, when considering the economics of the different layouts studied, the membrane area needed is the main parameter that can determine the convenience of the system. For this reason, higher pressure in the retentate side should be preferred, even if the corresponding efficiency is slightly lower. Concerning the biogas composition, this preliminary analysis showed how AD and LF are similar from an economic point of view: the first leads to a lower area of the membranes and to lower auxiliary electricity consumption, the second has a lower fuel cost and catalyst amount.

6. Conclusions

This paper discussed a detailed techno-economic assessment of an innovative system for hydrogen production from biogas. The innovation consists of using Palladium membrane in the reforming reactor for simultaneous hydrogen production and separation. This concept has been developed within BIONICO project. The performance of the BIONICO concept are compared against two commercially available technologies based on reforming, water gas shift reactors and pressure swing adsorption for hydrogen purification.

The system simulations performed with Aspen considered two different biogas compositions, featuring typical landfill and anaerobic digestion cases, to assess the impact on overall system design, performance and costs.

The BIONICO system outperforms the reference cases by 40–50% achieving a hydrogen production efficiency around 69% assuming a delivery pressure of 20 bar. In addition, the membrane reactor operates at lower temperature and pressure of the reference cases.

Between the two permeate side configurations investigated, sweep gas and vacuum pump, the former is penalized by the low hydrogen partial pressure in the feed side and the limited amount of sweep flowrate available. The resulting system efficiency and membrane for the sweep cases were 15% lower and at least 5 times larger than the vacuum pump ones.

Afterwards, the economic assessment for the investigated cases was carried out accounting for both the capital and operating costs to determine the hydrogen production costs. The hydrogen cost production of the BIONICO case at 20 bar ranges from 4 to 4.1 €/kg_{H2}, while the reference case resulted 4.21 €/kg_{H2} and 6.4 €/kg_{H2} for the SR and ATR respectively. With respect to the steam reforming reference case, the BIONICO one has lower biogas and capital costs, but higher electricity costs (as consequence of the hydrogen compression consumptions), while it has lower biogas and electricity cost with respect to the ATR case. Between the landfill and anaerobic digestion cases, the latter has the lower costs as consequence of the higher methane content and same price assumed.

These results outline that membrane reactors are a promising technology for green hydrogen production starting from biogas.

Table 9
O&M fixed and variable costs.

Components	units	Cost
Catalyst	k€/m^3	540 (Lifetime 5 y)
Filler particles	k€/m^3	50 (Lifetime 5 y)
Deionisation Resin	€/y	447 (Lifetime 5 y)
Landfill Biogas [44]	€/GJ	1.50
Anaerobic Digester [44]	€/GJ	3.46
Electric energy [45]	€/kWh	0.12
Process water	€/m^3	0.35
Maintenance	–	2% TPC
Insurance	–	2.5% TPC
Labour cost	€	60000

Table 10
Total Plant Cost of BIONICO layouts at different operating conditions.

BG composition	Cost (k€)				
	LF	LF	LF	AD	AD
P_{feed} / P_{perm}	12/0.1	10/0.1	20/1.1	12/0.1	12/0.2
Reforming Reactor (and membrane)	24.8	28.1	78.3	21.7	34.4
Heat Exchangers	27.9	27.8	38.0	29.8	31.8
Biogas Compressor	3.4	3.2	5.1	2.7	2.7
Air Compressor/Fan	0.1	0.1	0.1	0.1	0.1
Water Demi + Pump	1.1	1.1	2.5	1.1	1.1
Vacuum Pump + H_2 compressor @ 20 bar	8.4	8.4	4.4	8.4	8.0
Burner	5.0	5.0	5.0	5.0	5.0
TPC (@ 20 bar)	148.3	154.4	279.9	144.2	174.3
H_2 compressor @ 700 bar	22.1	22.1	22.1	22.1	22.1
TPC (@ 700 bar)	194.6	200.7	326.2	190.5	220.6

Table 11
O&M variable costs of the different layouts considered.

BG composition	O&M variable costs (k€/y)				
	LF	LF	LF	AD	AD
P_{feed} / P_{perm}	12/0.1	10/0.1	20/1.1	12/0.1	12/0.2
Catalyst	1.77	2.42	5.32	2.12	2.10
Membranes	3.81	4.51	13.02	3.48	5.51
Biogas	7.38	7.44	10.66	5.59	5.69
Deionisation resin	0.45	0.45	0.45	0.45	0.45
Electric energy @ 20 bar	24.62	23.85	20.65	23.96	22.30
Electric energy @ 700 bar	36.29	35.53	32.32	35.63	33.98
Water cost	0.05	0.05	0.17	0.05	0.05
O&M var. total @ 20 bar	38.07	38.71	50.26	35.64	36.10
O&M var. total @ 700 bar	49.75	50.39	61.94	47.32	47.78

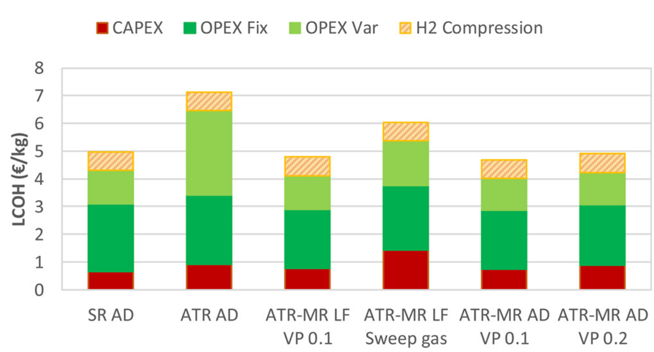

Fig. 13. Comparison of levelized cost of hydrogen between BIONICO and conventional system.

Acknowledgments

The BIONICO project leading to this application has received funding from the Fuel Cells and Hydrogen 2 Joint Undertaking under grant agreement no. 671459. This Joint Undertaking receives support from the European Union's Horizon 2020 research and innovation programme, Hydrogen Europe and N.ERGHY.

References

[1] M. Ball, M. Wietschel, The Hydrogen Economy: Opportunities and Challenges, Cambridge University Press, 2009.
[2] V. Sumbramani, A. Basile, N.T. Verizoglu, Compendium of Hydrogen Energy: Hydrgoen Production and Purification, (2015).
[3] P. Nikolaidis, A. Poullikkas, A comparative overview of hydrogen production processes, Renew. Sustain. Energy Rev. 67 (2017) 597–611, http://dx.doi.org/10.1016/j.rser.2016.09.044.
[4] S.E. Hosseini, M.A. Wahid, Hydrogen production from renewable and sustainable energy resources: promising green energy carrier for clean development, Renew. Sustain. Energy Rev. 57 (2016) 850–866, http://dx.doi.org/10.1016/j.rser.2015.12.112.
[5] I. Dincer, C. Acar, Review and evaluation of hydrogen production methods for better sustainability, Int. J. Hydrogen Energy 40 (2015) 11094–11111, http://dx.doi.org/10.1016/j.ijhydene.2014.12.035.
[6] U. Albrecht, M. Altmann, F. Barth, U. Bünger, D. Fraile, J.-C. Lanoix, E. Pschorr-Schoberer, W. Vanhoudt, W. Weindorf, M. Zerta, W. Zittel, Study on Hydrogen from Renewable Resources in the EU Final Report, (2015), http://dx.doi.org/10.1017/CBO9781107415324.004.
[7] EurObserv'ER, The State of Renewable Energies in Europe, (2016) http://www.eurobserv-er.org/pdf/bilan11.asp.
[8] L.B. Braga, J.L. Silveira, M.E. da Silva, C.E. Tuna, E.B. Machin, D.T. Pedroso, Hydrogen production by biogas steam reforming: a technical, economic and ecological analysis, Renew. Sustain. Energy Rev. 28 (2013) 166–173, http://dx.doi.org/10.1016/j.rser.2013.07.060.
[9] H.J. Alves, C. Bley Junior, R.R. Niklevicz, E.P. Frigo, M.S. Frigo, C.H. Coimbra-Araújo, Overview of hydrogen production technologies from biogas and the applications in fuel cells, Int. J. Hydrogen Energy 38 (2013) 5215–5225, http://dx.doi.org/10.1016/j.ijhydene.2013.02.057.
[10] T. Ohkubo, Y. Hideshima, Y. Shudo, Estimation of hydrogen output from a full-scale plant for production of hydrogen from biogas, Int. J. Hydrogen Energy 35 (2010) 13021–13027, http://dx.doi.org/10.1016/j.ijhydene.2010.04.063.
[11] J.D. Holladay, J. Hu, D.L. King, Y. Wang, An overview of hydrogen production technologies, Catal. Today 139 (2009) 244–260, http://dx.doi.org/10.1016/j.cattod.2008.08.039.
[12] K. Göransson, U. Söderlind, J. He, W. Zhang, Review of syngas production via biomass DFBGs, Renew. Sustain. Energy Rev. 15 (2011) 482–492, http://dx.doi.org/10.1016/j.rser.2010.09.032.
[13] P. Ugarte, P. Durán, J. Lasobras, J. Soler, M. Menéndez, J. Herguido, Dry reforming of biogas in fluidized bed: process intensification, Int. J. Hydrogen Energy. 42 (2017) 13589–13597, http://dx.doi.org/10.1016/j.ijhydene.2016.12.124.
[14] G. Di Marcoberardino, D. Vitali, F. Spinelli, M. Binotti, G. Manzolini, Green hydrogen production from raw biogas: a techno-economic investigation of conventional processes using pressure swing adsorption unit, Processes 6 (2018).
[15] S.N. Paglieri, J.D. Way, Innovations in palladium membrane research, Sep. Purif. Rev. 31 (2002) 1–169, http://dx.doi.org/10.1081/SPM-120006115.
[16] E. Fernandez, A. Helmi, K. Coenen, J. Melendez, J.L. Viviente, D.A. Pacheco Tanaka, M. van Sint Annaland, F. Gallucci, Development of thin Pd–Ag supported membranes for fluidized bed membrane reactors including WGS related gases, Int. J. Hydrogen Energy 40 (2015) 3506–3519, http://dx.doi.org/10.1016/j.ijhydene.2014.08.074.
[17] F. Gallucci, E. Fernandez, P. Corengia, M. van Sint Annaland, Recent advances on membranes and membrane reactors for hydrogen production, Chem. Eng. Sci. 92 (2013) 40–66, http://dx.doi.org/10.1016/j.ces.2013.01.008.
[18] L. Roses, F. Gallucci, G. Manzolini, S. Campanari, M. van Sint Annaland, Comparison between fixed bed and fluidized bed membrane reactor configurations for PEM based micro-cogeneration systems, Chem. Eng. J. 171 (2011) 1415–1427, http://dx.doi.org/10.1016/j.cej.2011.05.061.
[19] Binotti, et al., Biogas Membrane Reformer for Decentralized H2 Production, (2015) http://www.bionicoproject.eu/.
[20] J.M. Vásquez Castillo, T. Sato, N. Itoh, Effect of temperature and pressure on hydrogen production from steam reforming of biogas with Pd-Ag membrane reactor, Int. J. Hydrogen Energy 40 (2015) 3582–3591, http://dx.doi.org/10.1016/j.ijhydene.2014.11.053.
[21] F.S.A. Silva, M. Benachour, C.A.M. Abreu, Evaluating hydrogen production in biogas reforming in a membrane reactor, Braz. J. Chem. Eng. 32 (2015) 201–210, http://dx.doi.org/10.1590/0104-6632.20150321s00002820.
[22] N.C.A. de Nooijer, F. Gallucci, E. Pellizzari, J. Melendez, D.A. Pacheco Tanaka, G. Manzolini, M. van Sint Annaland, On concentration polarisation in a fluidized bed membrane reactor for biogas steam reforming: modelling and experimental validation, Chem. Eng. J. 348 (2018) 232–243, http://dx.doi.org/10.1016/j.cej.2018.04.205.
[23] AspenTech, Aspen Plus, (n.d.). http://www.aspentech.com/products/aspen-plus.aspx.
[24] S. Foresti, G. Manzolini, Performances of a micro-CHP system fed with bio-ethanol based on fluidized bed membrane reactor and PEM fuel cells, Int. J. Hydrogen Energy 41 (2016) 9004–9021, http://dx.doi.org/10.1016/j.ijhydene.2016.03.210.
[25] G. Di Marcoberardino, G. Manzolini, Investigation of a 5 kW micro-CHP PEM fuel cell based system integrated with membrane reactor under EU natural gas quality, Int. J. Hydrogen Energy 42 (2017) 13988–14002, http://dx.doi.org/10.1016/j.ijhydene.2017.02.016.
[26] G. Di Marcoberardino, L. Roses, G. Manzolini, Technical assessment of a micro-cogeneration system based on polymer electrolyte membrane fuel cell and fluidized bed autothermal reformer, Appl. Energy 162 (2016) 231–244, http://dx.doi.org/10.1016/j.apenergy.2015.10.068.
[27] D.Y. Peng, D.B. Robinson, New two-constant equation of state, Ind Eng. Chem. Fundam. 15 (1976) 59–64.
[28] H.G. Rackett, Equation of state for saturated liquids, J. Chem. Eng. Data. 15 (1970) 514–517 http://www.scopus.com/inward/record.url?eid=2-s2.0-33947293984&partnerID=tZOtx3y1.
[29] L. Haar, J. Gallagher, G.S. Kell, NBS/NRC Steam Tables: Thermodynamic and Transport Properties and Computer Programs for Vapor and Liquid States of Water in S.I. Units, Hemisphere Publishing Corporation, Washington, 1984.
[30] ENC, Personal Communication (2016).
[31] G. Di Marcoberardino, F. Gallucci, G. Manzolini, M. van Sint Annaland, Definition

of validated membrane reactor model for 5 kW power output CHP system for different natural gas compositions, Int. J. Hydrogen Energy 41 (2016) 19141–19153, http://dx.doi.org/10.1016/j.ijhydene.2016.07.102.
[32] S. Foresti, G. Di Marcoberardino, G. Manzolini, N. De Nooijer, F. Gallucci, M. van Sint Annaland, A comprehensive model of a fluidized bed membrane reactor for small-scale hydrogen production, Chem. Eng. Process. - Process Intensif. 127 (2018) 136–144, http://dx.doi.org/10.1016/J.CEP.2018.01.018.
[33] D. Kunii, O. Levenspiel, Fluidization Engineering, 2nd ed., Butterworth-Heinemann, 1991.
[34] K. Numaguchi, Kikuchi T, Intrinsic kinetics and design simulation in a complex reaction network; steam-methane reforming, Chem. Eng. Sci. 43 (1988) 2295–2301.
[35] L. Ma, D.L. Trimm, C. Jiang, The design and testing of an autothermal reactor for the conversion of light hydrocarbons to hydrogen I. The kinetics of the catalytic oxidation of light hydrocarbons, Appl. Catal. A Gen. 138 (1996) 275–283.
[36] V. Chiodo, S. Maisano, G. Zafarana, F. Urbani, Effect of pollutants on biogas steam reforming, Int. J. Hydrogen Energy 42 (2017) 1622–1628, http://dx.doi.org/10.1016/J.IJHYDENE.2016.07.251.
[37] G. Rabenstein, V. Hacker, Hydrogen for fuel cells from ethanol by steam-reforming, partial-oxidation and combined auto-thermal reforming: a thermodynamic analysis, J. Power Sources 185 (2008) 1293–1304, http://dx.doi.org/10.1016/J.JPOWSOUR.2008.08.010.
[38] E. Fernandez, A. Helmi, J.A. Medrano, K. Coenen, A. Arratibel, J. Melendez, N.C.A. de Nooijer, V. Spallina, J.L. Viviente, J. Zuñiga, M. van Sint Annaland, D.A. Pacheco Tanaka, F. Gallucci, Palladium based membranes and membrane reactors for hydrogen production and purification: an overview of research activities at Tecnalia and TU/e, Int. J. Hydrogen Energy 42 (2017) 13763–13776, http://dx.doi.org/10.1016/j.ijhydene.2017.03.067.
[39] F. Gallucci, J.A. Medrano, E. Fernandez, J. Melendez, Mvan S. Annaland, Advances on High temperature Pd-based membranes and membrane reactors for hydrogen purification and production graphical abstract keywords, J. Membr. Sci. Res. 3 (2017) 142–156, http://dx.doi.org/10.22079/jmsr.2017.23644.
[40] J. Melendez, N. de Nooijer, K. Coenen, E. Fernandez, J.L. Viviente, M. van Sint Annaland, P.L. Arias, D.A.P. Tanaka, F. Gallucci, Effect of Au addition on hydrogen permeation and the resistance to H2S on Pd-Ag alloy membranes, J. Memb. Sci. 542 (2017) 329–341, http://dx.doi.org/10.1016/J.MEMSCI.2017.08.029.
[41] G. Di Marcoberardino, L. Roses, G. Manzolini, Technical assessment of a micro-cogeneration system based on polymer electrolyte membrane fuel cell and fluidized bed autothermal reformer, Appl. Energy 162 (2016), http://dx.doi.org/10.1016/j.apenergy.2015.10.068.
[42] K. Gerdes, W.M. Summers, J. Wimer, Cost Estimation Methodology for NETL Assessments of Power Plant Performance DOE/NETL-2011/1455, 2011, 26. http://www.netl.doe.gov/File Library/research/energy analysis/publications/QGESSNETLCostEstMethod.pdf.
[43] FERRET, A Flexible Natural Gas Membrane Reformer for M-CHP Applicatins, (2014) http://www.ferret-h2.eu.
[44] International Renewable Energy Agency (IRENA), Biomass for Power Generation, (2012).
[45] European Commission, EuroStat, Statistics Explained, (2015) http://ec.europa.eu/eurostat/statistics-explained/index.php/Main_Page.